



STATE UNIVERSITY OF NEW YORK
AT STONY BROOK

COLLEGE OF
ENGINEERING

Report No. 58

AXISYMMETRICAL TURBULENT SWIRLING

NATURAL CONVECTION PLUME

PART II - EXPERIMENTAL INVESTIGATION

by

Richard Shao-lin Lee

(Shao-lin Lee)

November 1965

Spec

TAI

N532

No. 58

C-2

AXISYMMETRICAL TURBULENT SWIRLING
NATURAL CONVECTION PLUME
PART II - EXPERIMENTAL INVESTIGATION

By

Richard Shao-lin Lee
(Shao-lin Lee)
Associate Professor
Department of Mechanics
State University of New York at Stony Brook

ABSTRACT

An experimental investigation is made of the behavior of an axisymmetrical turbulent swirling natural convection plume in an otherwise motionless ambient fluid. The swirling plume is issued from the exit of a swirling plume generator which couples the hot gases from a Bunsen burner flame and the swirling mass of air from a ring of distributed tangential jets. Temperature and velocity fields of the swirling plume are measured by the use of a temperature-calibrated, V-shaped hot-wire probe. Measured results of the vertical and swirling velocities, the temperature, and the characteristic radius of the swirling plume are found to agree closely with the theoretical predictions of Part I.

INTRODUCTION

The phenomenon of a turbulent swirling natural convection plume itself is not a new one, but only recently, as a result of the current interest in the further understanding of the behavior of a free-burning diffusion flame in the atmosphere, has it come under intensive examination.

A free-burning diffusion flame releases thermal energy due to chemical reactions which heat up the products of combustion as well as some amount of the entrained ambient air. The hot gases have smaller densities than their unheated counterparts and the related buoyancy force will lift them upward in the direction directly above the flame to form a natural convection plume. The natural convection plume in turn will induct fresh air and fuel into the combustion zone of the flame for further combustion. The behavior of a free-burning diffusion flame is therefore closely related to that of a natural convection plume in a very sensitive way. It is clear that a thorough understanding of the behavior of the related natural convection plume will most hopefully reveal some of the so far rather mysterious behavior of a free-burning diffusion flame in the atmosphere.

In an unobstructed atmosphere, the induced air will move directly toward the axis of the flame-plume structure while in the meantime its direction of motion will be lifted upward when its temperature is

raised due to either being heated by or mixing with the hotter gases from the flame-plume structure. The flame will have a familiar appearance such as that of a candle flame or a nice steady flame from a Bunsen burner. On the other hand it has just recently come to light that the appearance of the flame will be changed drastically when some amount of circulation is introduced in the ambient atmosphere either by employing a ring of directional vanes to guide the inducted air or by rotating a vertical circular screen coaxial with the flame as reported by Emmons (1965) [1]. The air inducted into the flame will move toward the flame axis along a spiral path as viewed from its projection on a horizontal plane while in the meantime its direction of motion will be lifted upward when its temperature is raised due to either being heated by or mixing with the hotter gases from the flame. The flame will shrink in cross-sectional size but will stretch longitudinally many times its normal length. The appearance of the flame gives the indication of a sizeable amount of swirl induced in the flame. Consequently, it becomes evident that the plume above such a flame will also have a certain amount of swirl even though the atmosphere surrounding the plume may be set to be unobstructed for the entire length of the plume.

The axisymmetrical turbulent non-swirling natural convection plume has been in the past studied quite thoroughly, both theoretically and experimentally, and the results can be considered as quite satisfactory. The theoretical analyses are reported separately in the works of Morton, Taylor and Turner (1956) [2] and Morton (1959) [3, 4], both of which

employ the assumption of the lateral entrainment of the ambient fluid first introduced by Taylor (1945) [5]. The experimental findings are reported in the work of Rouse, Yih and Humphreys (1952) [6]. The agreement between the theoretical analyses and the corresponding experimental findings is found to be very close.

The axisymmetrical turbulent swirling natural convection plume has never been analyzed until most recently. Lee (1965) [7] studied the behavior of such a plume in an otherwise motionless, unobstructed ambient atmosphere by the use of the Karman integral method. With the introduction of the assumption of similar axial and swirling velocity profiles and similar buoyancy profile, and the assumption of lateral entrainment of ambient fluid, the complexity of the problem was greatly reduced. The behavior of the swirling plume was found to depend solely on two physical parameters associated with the source characteristics, the source Froude number and the source swirling velocity parameter. A series solution developed in the vicinity of the source of the swirling plume was obtained for any values of these two physical parameters. Numerical solutions for extended range of axial distance from the source of the swirling plume and for wide ranges of selected representative values of these two physical parameters were obtained with the use of a digital electronic computer.

EXPERIMENTAL APPARATUS

The experimental apparatus consists of the following items

(A) The swirling plume generator.

The swirling plume generator, as shown in the sketch of Figure 1, is made of an 1-1/2 inch Bunsen burner fixed near the lower end of a vertical 11 inch long copper tube of 2 inch inside diameter, with a ring of evenly spaced horizontal tangential air jet inlets made of copper tubing 3/16 inch inside diameter coming into the 2 inch tube. The burner is lined up with the axis of the 2 inch copper tube and its top is fixed at a level 2 inches from the lower end and 9 inches from the upper end of the 2 inch copper tube. The bottom of the 2 inch copper tube is firmly sealed around the burner. The axes of the tangential air jet inlets are located in a horizontal plane at the level of the top of the burner. The primary air and propane gas fuel for combustion are previously mixed in a mixing chamber and then introduced into the Bunsen burner through a carefully metered passage. Secondary air for the generation of swirl is supplied through evenly spaced, horizontal, tangential air jets which receive compressed air from a distribution tank. Compressed air is furnished to the distribution tank from a compressed air main through a carefully metered passage. The vertical 2 inch copper tube forms a casing guiding the flow passage. A circular cylindrical coil of 1/4 inch copper tubing is wrapped around the vertical flow casing to form a cooling jacket for it. Cooling water is run through the coil to prevent the flow casing from being overheated.

(B) The cage.

The cage is a rectangular steel frame structure 6 feet long, 6 feet wide and 12 feet tall, located in the central portion of a large laboratory room. A horizontal asbestos platform with a 2 inch circular hole for the plume generator is set at a level about 3 feet above the floor and covers the whole horizontal cross section of the cage. The vertical surfaces of the cage are covered with a layer of No. 48 aluminum window screen to reduce the undesirable disturbances to the plume from the surrounding air. On top of the cage, a tapered metal hood is located to take away the excessive hot gases through a minimum-draft exhaust duct extending to the outside of the laboratory. Parallel to but 2 feet away from each side of the cage, a vertical baffle wall, 10 feet wide and extending from about 2 feet to about 8 feet above the floor, is set to further reduce the undesirable disturbances to the plume from the surrounding air.

A traverse mechanism for carrying the temperature and velocity measuring hot-wire probe is set on one side of the cage. This mechanism is capable of traveling up and down vertically from the level of the platform to a level approximately 60 inches above the platform and in and out horizontally covering the entire length of the cage. A protected slot is cut in the screen and in the baffle wall on the side of the traverse mechanism to make possible the motion of the mechanism. A couple of large observation glass windows are set in the baffle wall, one on each side of the traverse mechanism. A general view of the experimental cage is shown in Figure 2.

(C) The hot-wire probe.

For the velocity measurement, the conventional hot-wire probe has been found unreliable in much of the temperature range of the present swirling plume work. Furthermore, the hot wire will break up after its exposure to the hot gas stream for a relatively short period of time. However, if one is only interested in the measurement of the time-mean velocity instead of the detailed turbulence information of the flow, one can use a much heavier piece of wire, which will withstand the temperature, and require a much simpler accompanying electrical circuit. The hot-wire probe used in this investigation consists primarily of a V-shaped thin piece of resistance metal wire and a thermocouple. The hot wire is a piece of pure nickel wire, 0.002 inch in diameter and about 5/16 inch in total length, soldered to three stainless steel wire supports in a 60-degree V shape. A copper-constantan thermocouple is put slightly behind but directly above the hot wire. Since the velocities involved in the present plume work are extremely small and since the net radiation heat exchange between the thermocouple and surroundings is also very small, the thermocouple measures the local static temperature very closely. Furthermore, since in the temperature range encountered the thermocouple voltage is practically linearly related to the temperature, the local time-mean static temperature can be determined from the mean voltage reading. The probe can be remotely rotated around its axis which remains horizontal but perpendicular to the axis of the probe carriage of the traverse mechanism. In the V-shaped hot

wire probe a constant current of 0.6 amperes is maintained by a steady direct current source. The electrical potential changes at the three terminals are compared by an outside circuit, a sketch of which is shown in Figure 3. When the readings are properly calibrated against the local time-mean static temperature, the probe measures the magnitude and direction of the local time-mean velocity. The calibration of the probe is carried out with the aid of a calibration tunnel which produces an air stream of known velocity and temperature. A typical calibration chart is shown in Figure 4. All electrical potentials are recorded on a Speedo-max recorder. It should be noted, as seen from the typical calibration chart, that the response of the hot wire to the velocity of the gas stream can be considered locally linear over the velocity and temperature ranges covered by the calibration. Therefore, in the measurement of a gas stream, if the range of fluctuation is not very large, the mean value of the recorded electrical potential change will correspond fairly closely to the time-mean velocity of the gas stream.

EXPERIMENTAL PROCEDURE AND RESULTS

Disturbances in the ambient room air were maintained at a minimum and the constancy of the temperature of the ambient room air was checked continuously throughout any one run of the experiment. Essentially a steady state situation is achieved before taking temperature readings for primary air supply, propane gas fuel supply, secondary air supply and the cooling water exit. In all cases, the swirling flame always stayed

within the length of the vertical flow casing of the swirling plume generator, the exit of which was set flush with the top of the platform of the cage.

Let x' be the vertical distance from the level of the top of the platform and r be the horizontal distance away from the plume axis as shown in the definition sketch of Figure 5. The hot-wire probe is set at a selected level x' , first at a station $(x', 0)$ along the axis of the swirling plume and then, step by step, at stations (x', r) away from the axis of the swirling plume. At each station (x', r) of the hot-wire probe, measurements are made on the local time-mean static temperature $T(x', r)$ by a precalibrated potentiometer, on the direction of the local time-mean velocity by rotating the probe to an orientation corresponding to a null reading on a potentiometer comparing electrical potential drops across the two sections of the V-shaped hot wire, and on the change of the electrical potential difference across the two sections of the hot wire which corresponded to the local time-mean velocity. The magnitude of the local time-mean velocity was then read from the calibration chart of the probe by using the measured change of the electrical potential difference across the two sections of the hot wire and the measured local time-mean static temperature. The magnitudes of the local time-mean vertical velocity, $u(x', r)$, and the local time-mean swirling velocity, $w(x', r)$, were computed from the magnitude and direction of the local time-mean velocity. It should be added here that the turbulent swirling plume is a strongly fluctuating fluid motion and therefore some estimate of the accuracy of the measurements would seem to be in order. In general, the fluctuations

of both the velocity and the temperature fields are found to have a minimum at the plume axis, increase monotonically with the radial distance from the axis, reach a maximum near the edge of the plume, and vanish rapidly from there toward the ambient air. The level of fluctuations falls in the range of 10 per cent of the total measured value at the plume axis and in the range of as high as 100 per cent of the total measured value near the edge of the plume. For regions near the plume axis, the recorded velocity and temperature would be within the locally linear ranges of response of both the hot wire and the thermocouple. For regions away from the plume axis, although the fluctuations increase rapidly toward the edge of the plume, the measured velocity and temperature, on the contrary, both decrease very rapidly toward the edge of the plume. Hence, even for the most violently fluctuating region near the edge of the plume, the response of both the hot wire and the thermocouple still can be considered approximately locally linear and the mean values of the recorded quantities should correspond fairly closely to the time-mean velocity and temperature respectively. Furthermore, in the present plume problem over 80 per cent of either the total axial linear momentum flux or the total temperature increment flux across the plume can be estimated to be contributed by the portion of the gas confined within the region bounded by a radius half the plume radius. Therefore, in the computation of the total fluxes across the plume, the large fluctuations of measured quantities near the edge of the plume would not significantly affect the results.

The selected levels, x' , for the present experiment were $11^{-3/4}$,

13^{-3/4}, 15^{-3/4}, 19^{-3/4}, 23^{-3/4}, 27^{-3/4}, 31^{-3/4}, 35^{-3/4}, 39^{-3/4}, and 43^{-3/4} inches above the platform of the cage. The normalized local time-mean vertical velocity, $u(x', r)/u(x', 0)$, and the normalized local time-mean temperature increment over ambient temperature, $\Delta T(x', r)/\Delta T(x', 0)$, are plotted against the square of the horizontal distance, r^2 , for all selected levels in Figures 6-1 through 6-3. $\Delta T(x', r)$ is the local time-mean temperature increment $[T(x', r) - T_1]$ where T_1 is the ambient temperature. It is observed that straight lines are obtained for both the normalized local time-mean vertical velocity profile and the normalized local time-mean temperature increment profile in such plots. The profiles can be thus represented by the following Gaussian expressions:

$$\frac{u(x', r)}{u(x', 0)} = \exp \left\{ - \frac{r^2}{[b(x')]^2} \right\}$$

$$\frac{\Delta T(x', r)}{\Delta T(x', 0)} = \exp \left\{ - \frac{r^2}{[b'(x')]^2} \right\}$$

where $b(x')$ is the value of r at which the magnitude of the vertical velocity, $u(x', r)$, is $1/e$ of that of the axial vertical velocity, $u(x', 0)$, and $b'(x')$ is the corresponding value of r for the temperature increment profile. By comparing the magnitudes of $b(x')$ and $b'(x')$ at different selected levels, it is found that $b'(x')/b(x')$ assumes a value in the neighborhood of 1.16, a value obtainable by performing similar comparisons on the experimental results on non-swirling turbulent plume reported by

Rouse, Yih, and Humphreys (1952)[6]. We can designate this constant $\lambda = b'(x')/b(x') = 1.16$.

The normalized local time-mean swirling velocity, $w(x', r)/w(x')$, is plotted against the normalized horizontal distance, $r/b(x')$, with $b(x')$ obtained from the vertical velocity profile, for all selected levels in Figure 7. $w(x')$ is the maximum value of $w(x', r)$ at a certain selected level x' . It is quite clear that all the plotted points cluster around a curve of similar profile designated by $f(r/b)$. This similar swirling velocity profile and the aforementioned Gaussian similar vertical velocity profile and temperature increment profile will give without any doubt the support to the correctness of the physical model assumed and used in the theoretical analysis on the axisymmetrical turbulent swirling natural convection plume by Lee (1965)[7]. The results for the maximum axial velocity $u(x')$, the maximum swirling velocity $w(x')$, the maximum temperature $T(x')$, and the characteristic radius of the plume $b(x')$ are plotted against the vertical distance from the level of the top of the platform in Figure 8.

In order to compare the present experimental findings with the only theoretical analysis by Lee (1965) [7] (which will be called Part I from here on), it is necessary to select one of the selected levels in the experiment as the level of the swirling source for the turbulent swirling plume above. Since the experimental results at the lowest level, $x' = 11^{-3/4}$ inch, already agree with the very physical model adopted in the theoretical analysis, it is only logical to select the level of $x' = 11^{-3/4}$ inches as the

level of the source, $x = 0$ in the notation of Part I. For the reasons given in Part I, $\Delta T/T_1$ can be replaced by $\Delta\gamma/\gamma_1$ where $\Delta\gamma = g(\rho_1 - \rho)$ is the local buoyancy and $\gamma_1 = g\rho_1$, ρ_1 being the density of the ambient fluid. The value of the entrainment coefficient α can be assigned a value of 0.08 as supported by the comparison between the theoretical works by Morton, Taylor and Turner (1956) [2] and Morton (1959) [3, 4], and the experimental works by Rouse, Yih and Humphreys (1952) [6] on a turbulent non-swirling plume. The same value of α is also supported by a comparison between the theoretical work by Lee (1965) [8] and the experimental work by Rose (1962) [9] on a turbulent swirling jet.

The source characteristics corresponding to the source located at $x = 0$ ($x' = 11.3/4$ inches) are as follows:

$$u_o = 34.0 \text{ ft/sec.}$$

$$w_o = 4.62 \text{ ft/sec.}$$

$$b_o = 1.66 \text{ inches}$$

$$\Delta\gamma_o/\gamma_1 = \Delta T_o/T_1 = 93/(89 + 460) = 0.169$$

The swirling velocity profile constant k , as defined by Equation (14) of Part I is

$$k = \int_0^{\infty} I(r/b) \cdot (r/b) d(r/b)$$

where

$$I(r/b) = \int_{(r/b)}^{\infty} \frac{[f(r/b)]^2}{(r/b)} d(r/b) .$$

With the functional form of $f(r/b)$ represented graphically as shown in Figure 7, the value of k is evaluated to be 0.156 for the present problem.

With the above values of u_o , w_o , b_o , $\Delta\gamma_o/\gamma_1$, a , λ and k used, the values of the source Froude number F and the source swirling velocity parameter G as defined in Part I can be evaluated to be

$$F = a^{\frac{1}{2}} u_o / [\lambda g^{\frac{1}{2}} b_o^{\frac{1}{2}} (\Delta\gamma_o/\gamma_1)^{\frac{1}{2}}] = 9.5$$

$$G = 2k^{\frac{1}{2}} w_o / u_o = 0.107$$

The following transformation formula are obtained for the various dependent variables and the independent variable x following Equation (22) of

Part I:

$$X = 2ax / (b_o F^{\frac{4}{7}} G^{\frac{3}{7}}) = 0.0911 x$$

$$B = b / (b_o F^{\frac{4}{7}} G^{\frac{3}{7}}) = 0.57 b$$

$$U = u F^{\frac{6}{7}} G^{\frac{1}{7}} / u_o = 0.135 u$$

$$W = w F^{\frac{6}{7}} G^{\frac{8}{7}} / w_o = 0.1054 w$$

$$1/P = (\Delta\gamma_o/\gamma_1) F^{-\frac{2}{7}} G^{-\frac{5}{7}} / (\Delta\gamma/\gamma_1) = 243/\Delta T$$

where x and b are in inches, u and w are in feet per second, and ΔT is in degrees Fahrenheit.

The experimental results made non-dimensional by the above transformations are plotted in Figure 9 against the corresponding theoretical

results of Part I with $F = 9.5$ and $G = 0.107$ used. Close agreement between the theoretical and the experimental results is obtained.

For another plume, measurements were made of the velocity and temperature distributions for various levels, starting from $x' = 6$ inches, from the top of the platform of the cage. If the level of $x' = 6$ inches is selected as the level of the source ($x = 0$), the source characteristics can be evaluated to be the following:

$$u_o = 5.3 \text{ ft/sec.}$$

$$w_o = 0.72 \text{ ft/sec.}$$

$$b_o = 2.49 \text{ inches}$$

$$\Delta Y_o / Y_1 = 0.169$$

The associated swirling velocity profile constant k is, for this case, evaluated to be 0.162. And, then, the values of F and G are computed as follows:

$$F = 1.4$$

$$G = 0.109$$

The corresponding comparison between the experimental and the theoretical results is shown in Figure 10. Close agreement is again obtained.

ACKNOWLEDGEMENT

The author wishes to express his most sincere appreciation to the National Science Foundation for its generous support which has made this investigation possible.

REFERENCES

1. Emmons, H. W., "Fundamental Problems of the Freeburning Fire", Tenth International Symposium on Combustion, 951-961, 1965.
2. Morton, B. R., Taylor, G. I., and Turner, J. S., "Turbulent Gravitational Convection from Maintained and Instantaneous Sources", Proceedings of Royal Society of London, Vol. 234 A, 1-22, 1956.
3. Morton, B. R., "Forced Plumes", Journal of Fluid Mechanics, Vol. 5 Part 1, 151-153, 1959.
4. Morton, B. R., "The Ascent of Turbulent Forced Plumes in a Calm Atmosphere", International Journal of Air Pollution, Vol. 1, 184-197, 1959.
5. Taylor, G. I., "Dynamics of a Mass of Hot Gas Rising in Air", U. S. Atomic Energy Commission, MDDC-919, LADC-276, 1945.
6. Rouse, H., Yih, C. S., and Humphreys, H. W., "Gravitational Convection from a Boundary Source", Tellus, Vol. 4, No. 3, 201-209, 1952.
7. Lee, Shao-lin, "Axisymmetrical Turbulent Swirling Natural Convection Plume, Part I - Theoretical Investigation", submitted for publication, 1965.
8. Lee, Shao-lin, "Axisymmetrical Turbulent Swirling Jet", Journal of Applied Mechanics, Vol. 32, Series E, No. 2, 258-262, June 1965.
9. Rose, W. G., "A Swirling Round Turbulent Jet", Journal of Applied Mechanics, Vol. 29, Series E, 615-625, 1962.

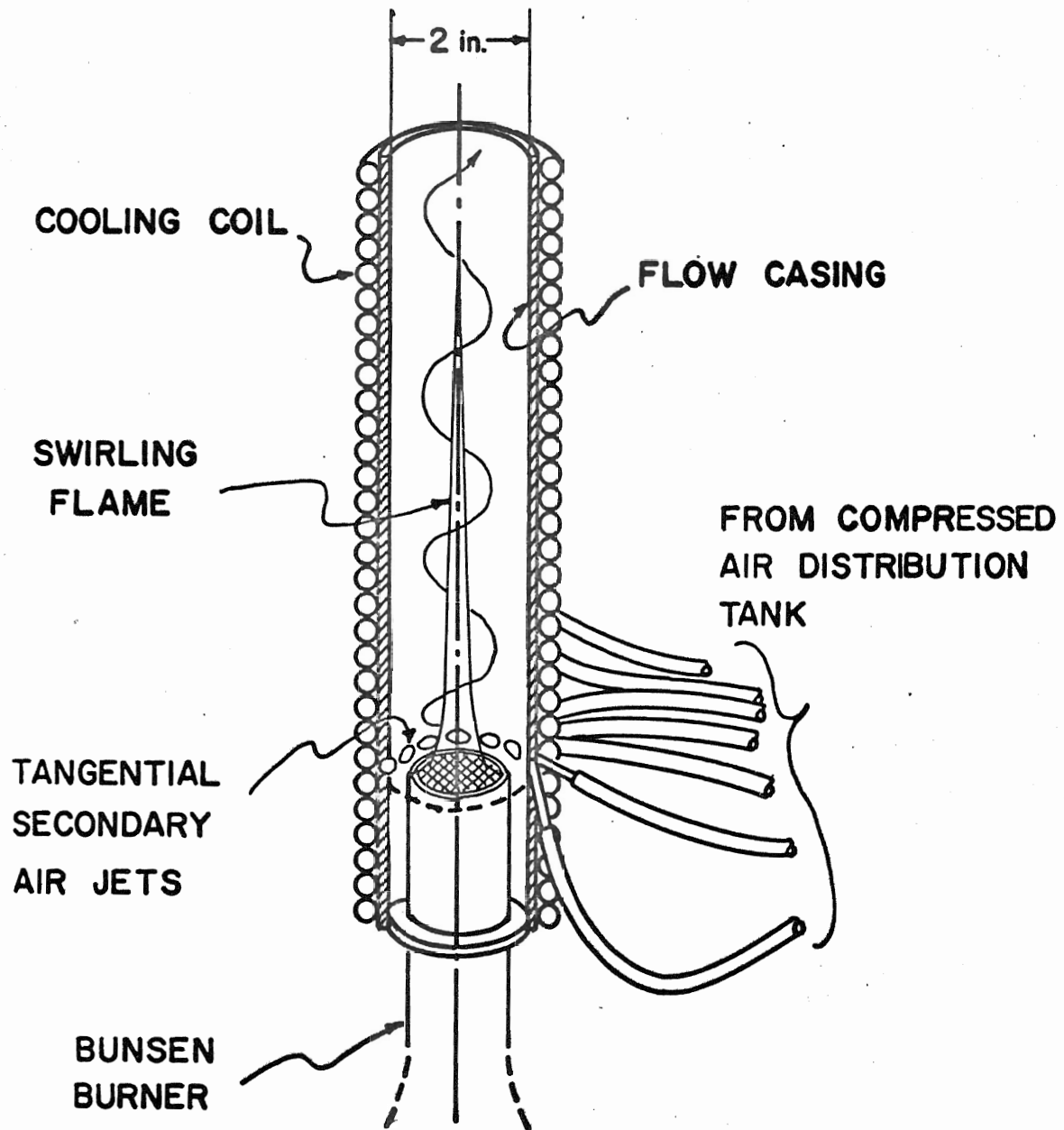


FIGURE I. SKETCH OF THE SWIRLING PLUME GENERATOR

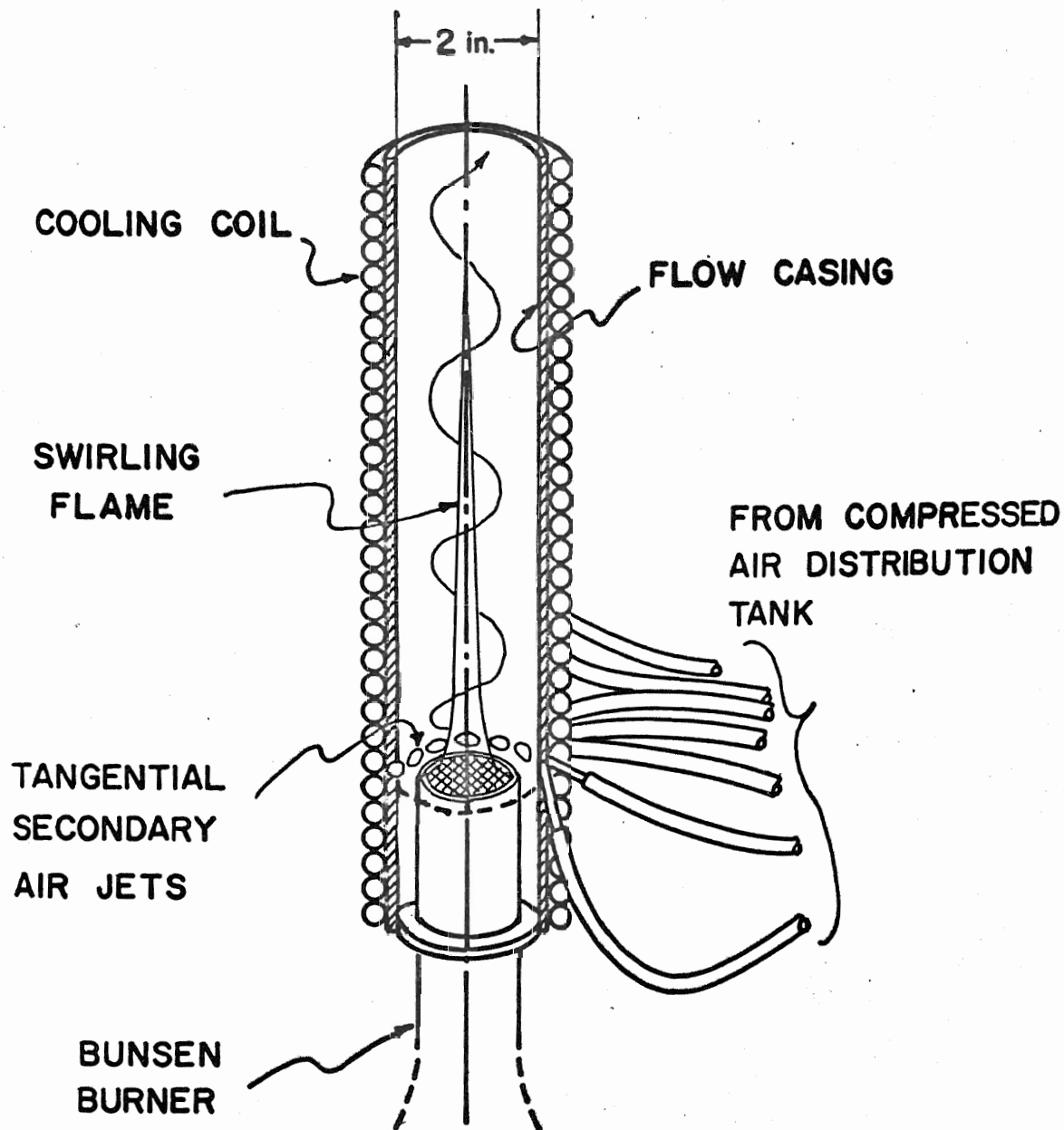


FIGURE 1. SKETCH OF THE SWIRLING PLUME GENERATOR

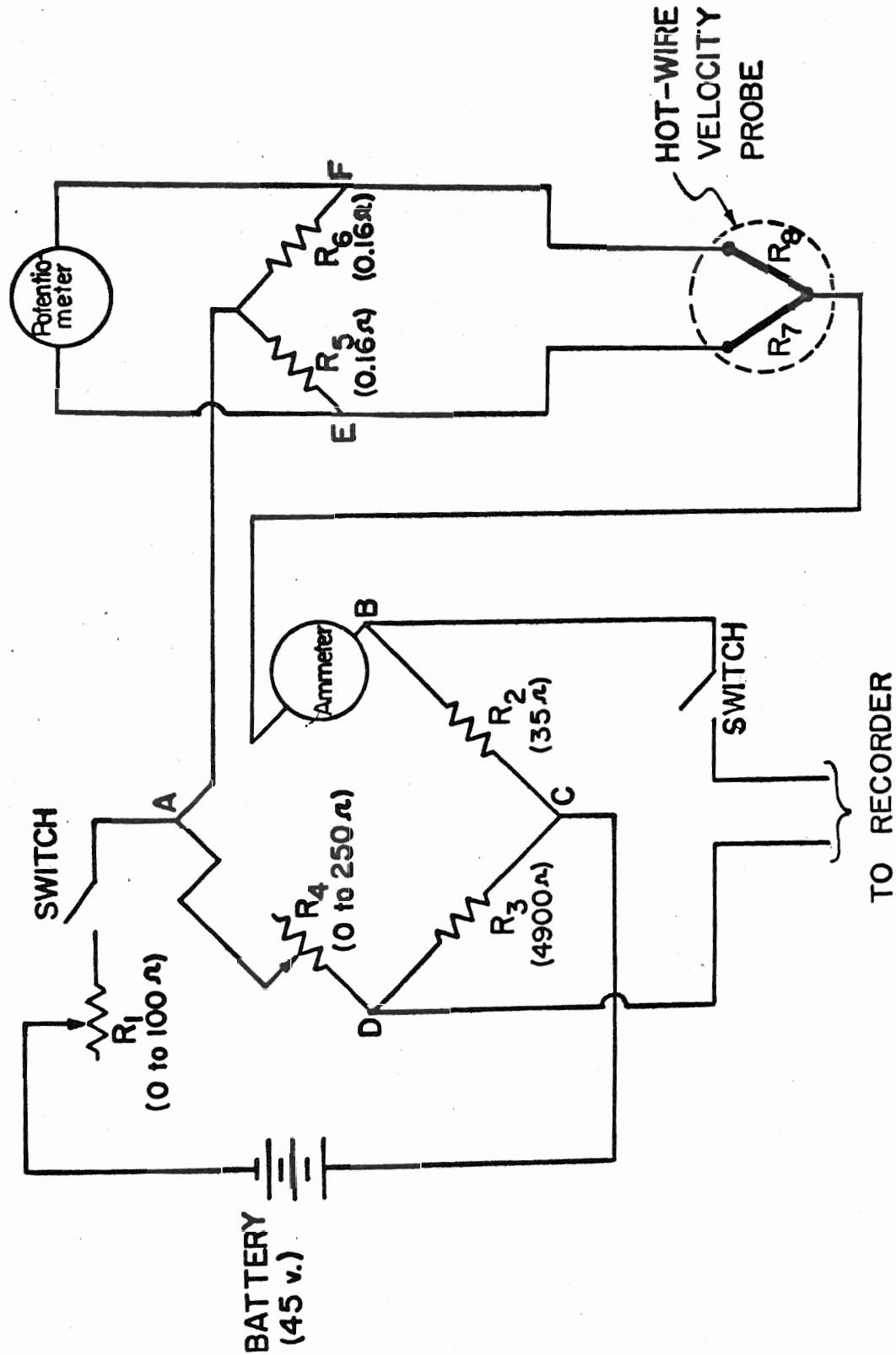


FIGURE 3. ANNEMOMETER CIRCUIT DIAGRAM

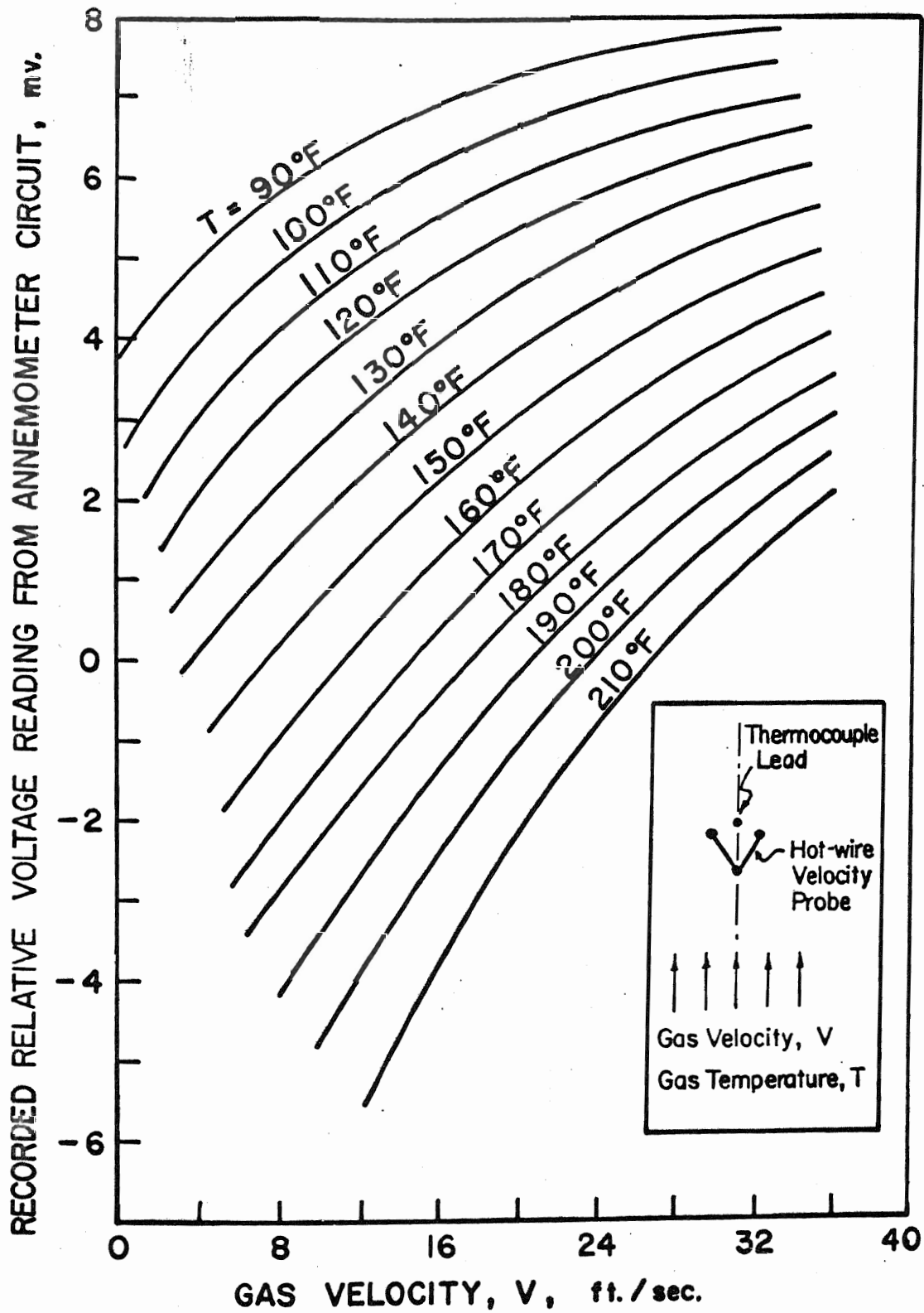


FIGURE 4. EXAMPLE OF CALIBRATION CHART FOR THE VELOCITY PROBE

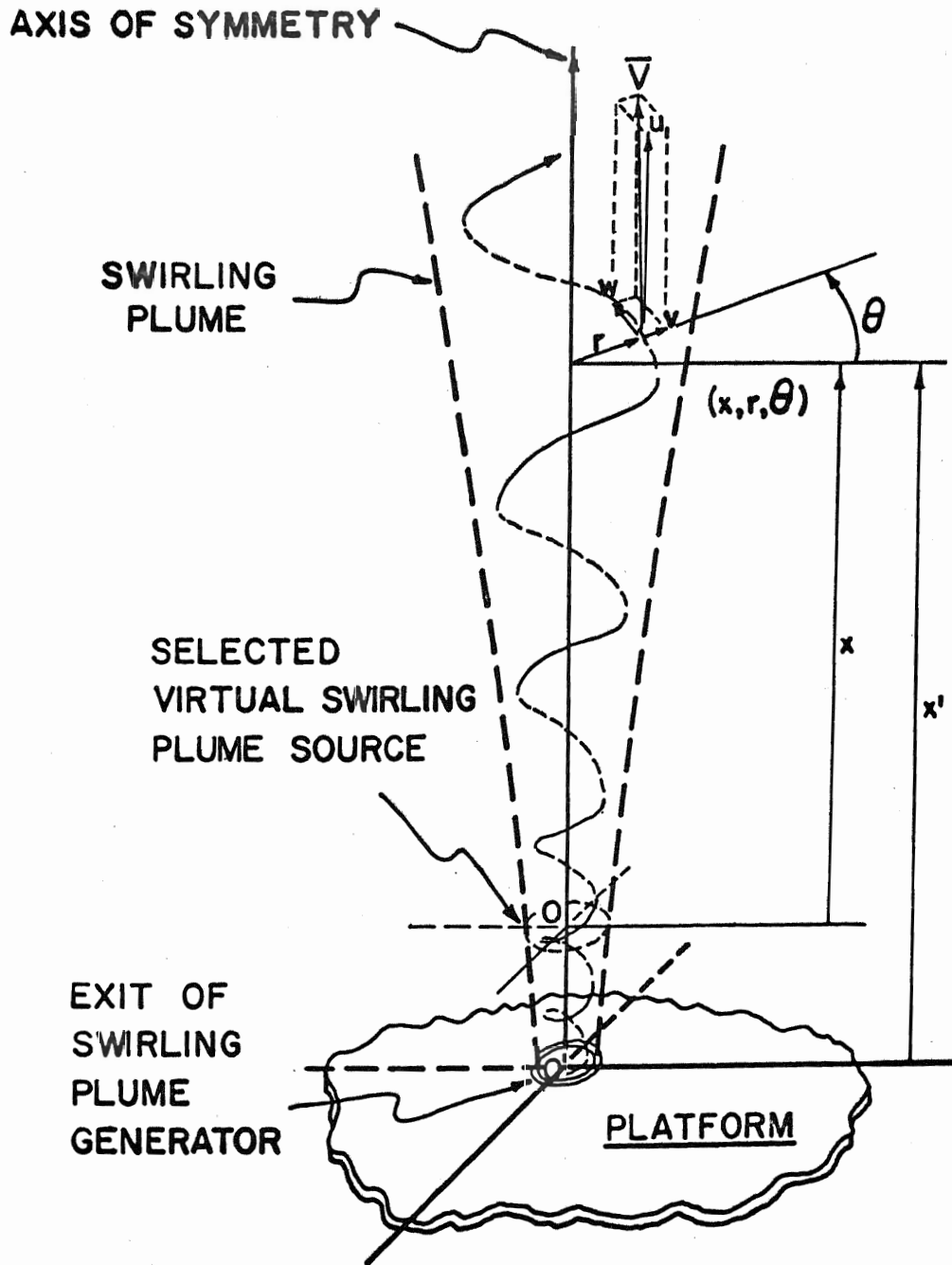


FIGURE 5. DEFINITION SKETCH

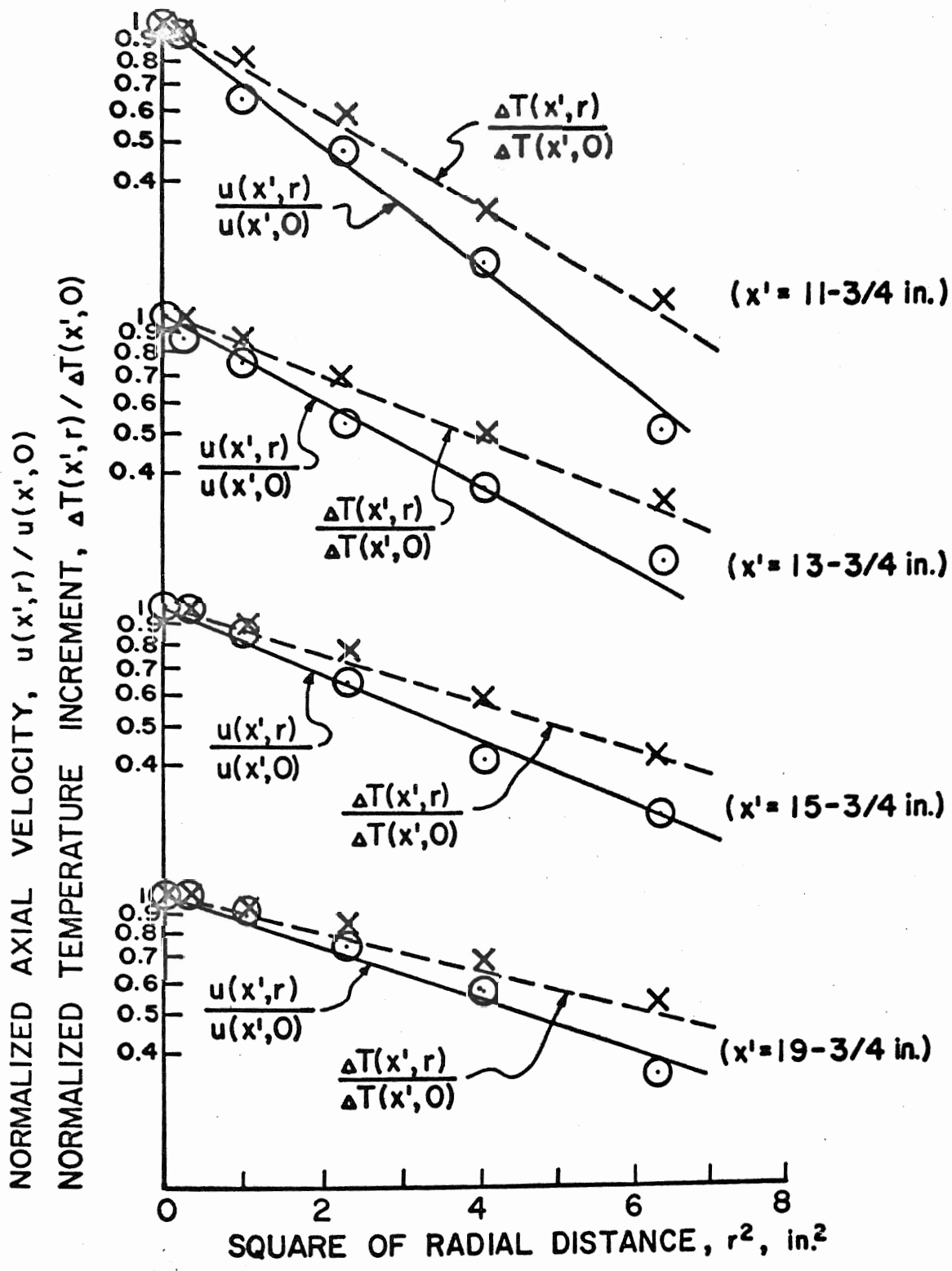


FIGURE 6-1. PLOTS OF AXIAL VELOCITY AND TEMPERATURE INCREMENT AGAINST SQUARE OF RADIAL DISTANCE AT FIXED HEIGHTS.

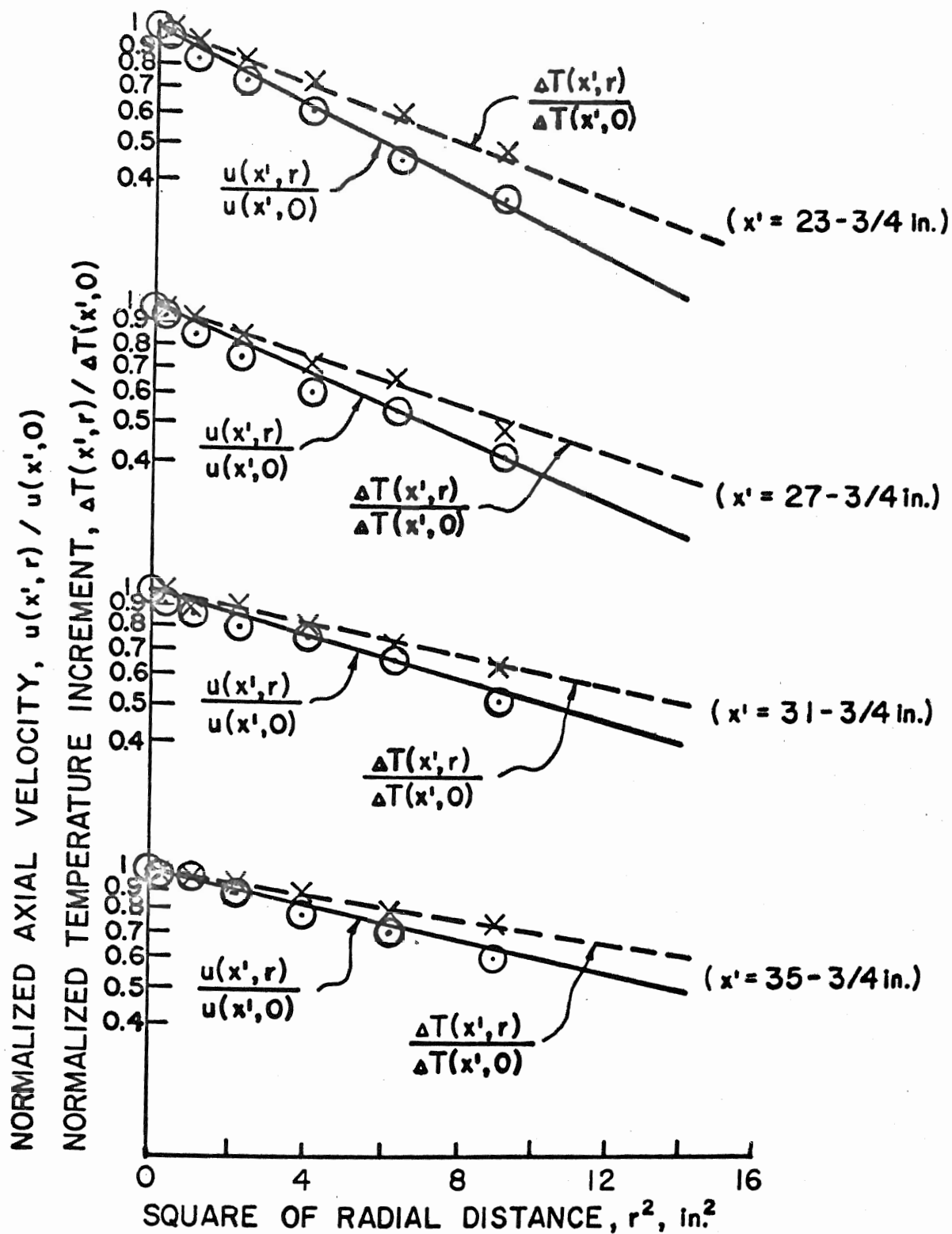


FIGURE 6-2. PLOTS OF AXIAL VELOCITY AND TEMPERATURE INCREMENT AGAINST SQUARE OF RADIAL DISTANCE AT FIXED HEIGHTS

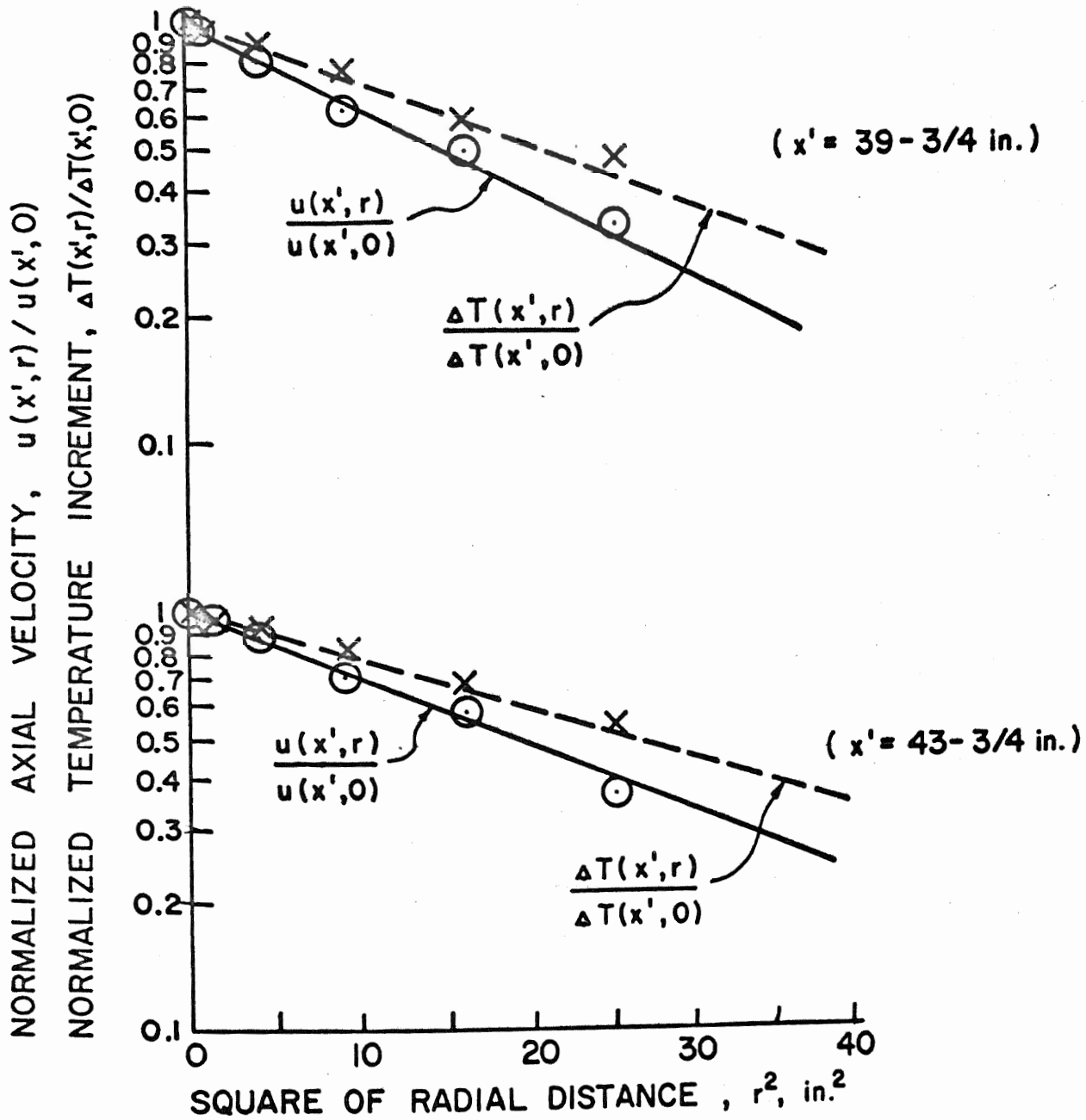


FIGURE 6-3. PLOTS OF AXIAL VELOCITY AND TEMPERATURE INCREMENT AGAINST SQUARE OF RADIAL DISTANCE AT FIXED HEIGHTS.

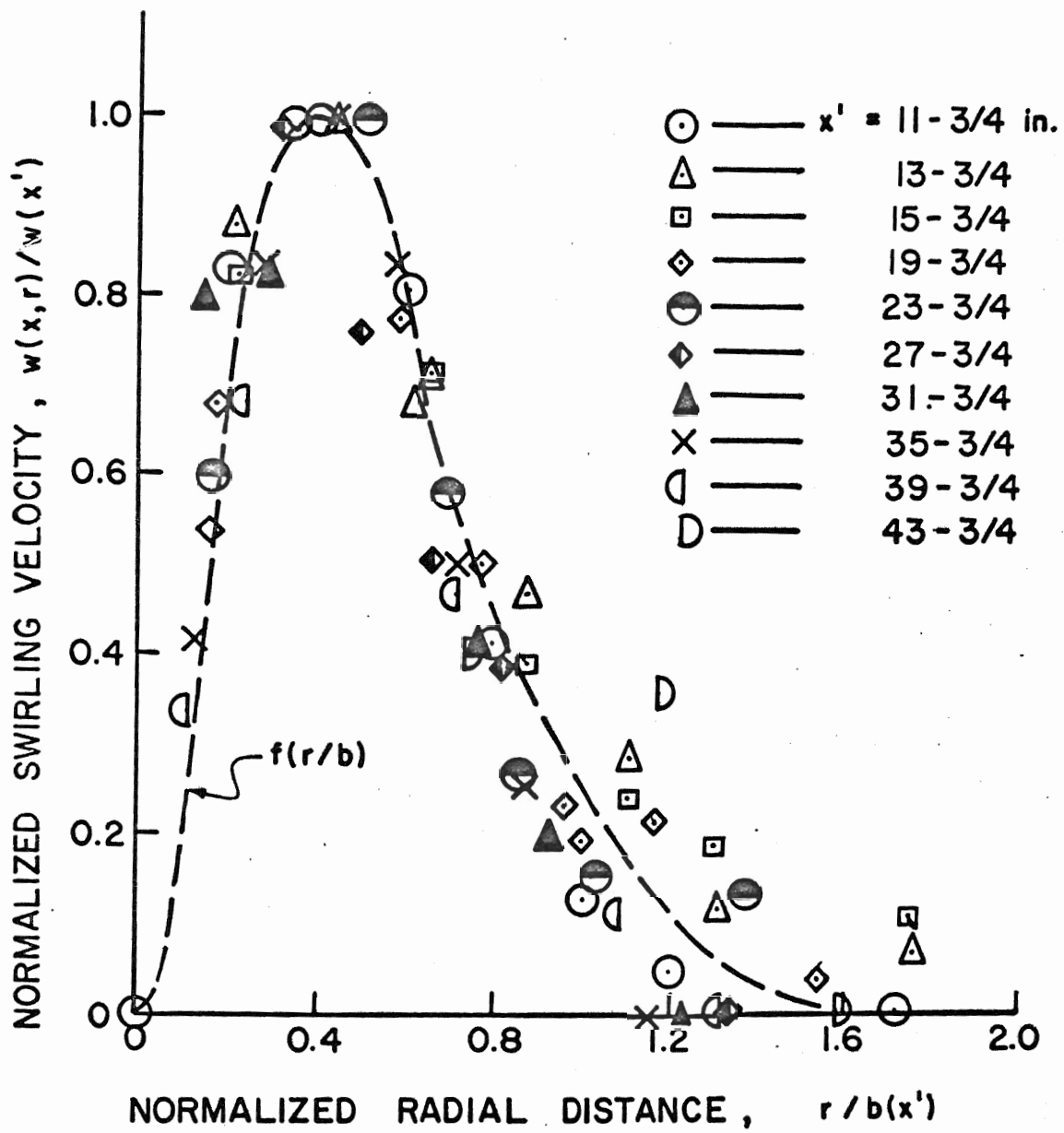


FIGURE 7. THE SWIRLING VELOCITY DISTRIBUTION

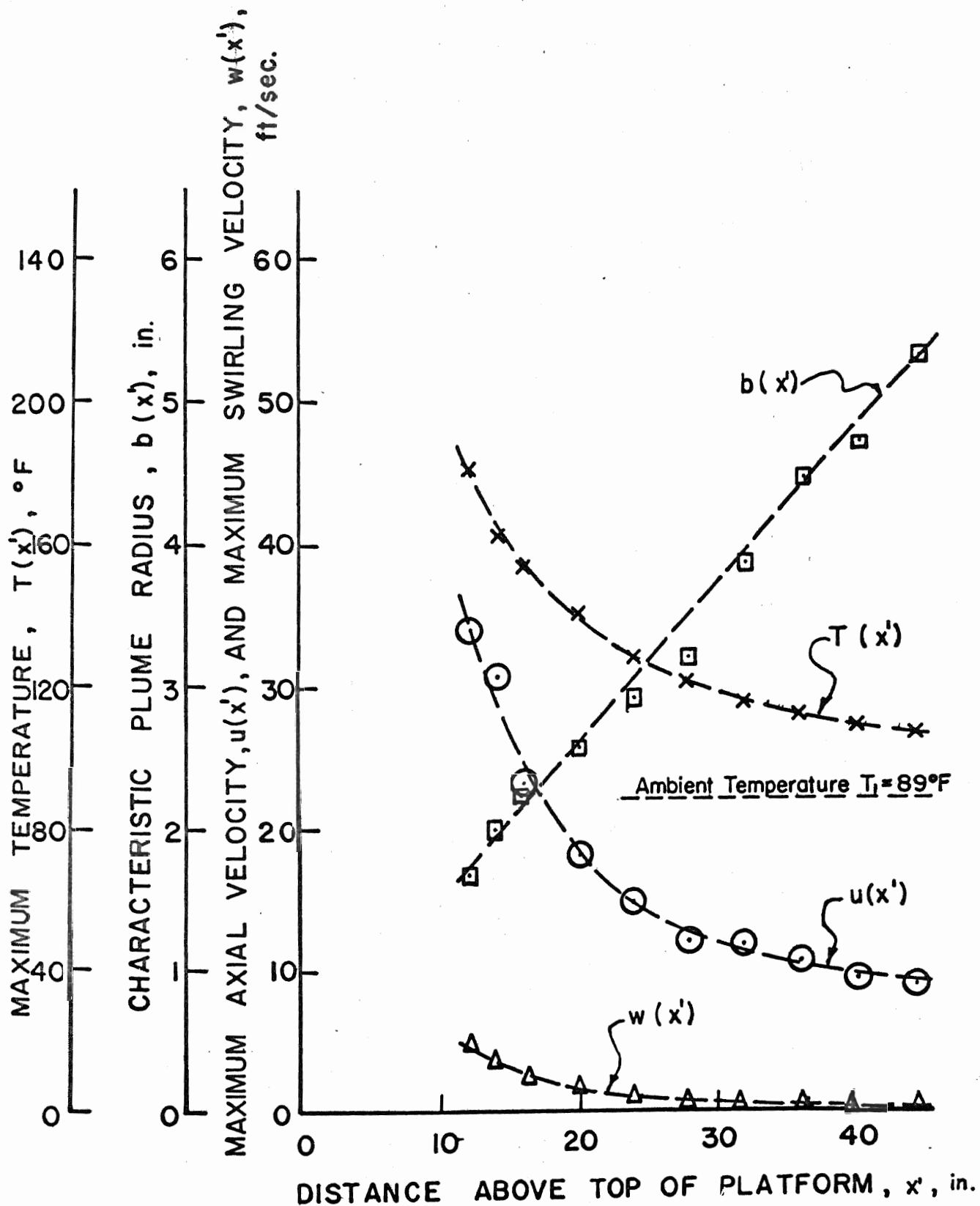


FIGURE 8. SUMMARIZED EXPERIMENTAL RESULTS

DIMENSIONLESS RECIPROCAL OF MAXIMUM BUOYANCY DIVIDED BY FOUR, DIMENSIONLESS MAXIMUM SWIRLING VELOCITY MULTIPLIED BY TEN, $(1/P)/4$ DIMENSIONLESS MAXIMUM AXIAL VELOCITY, U

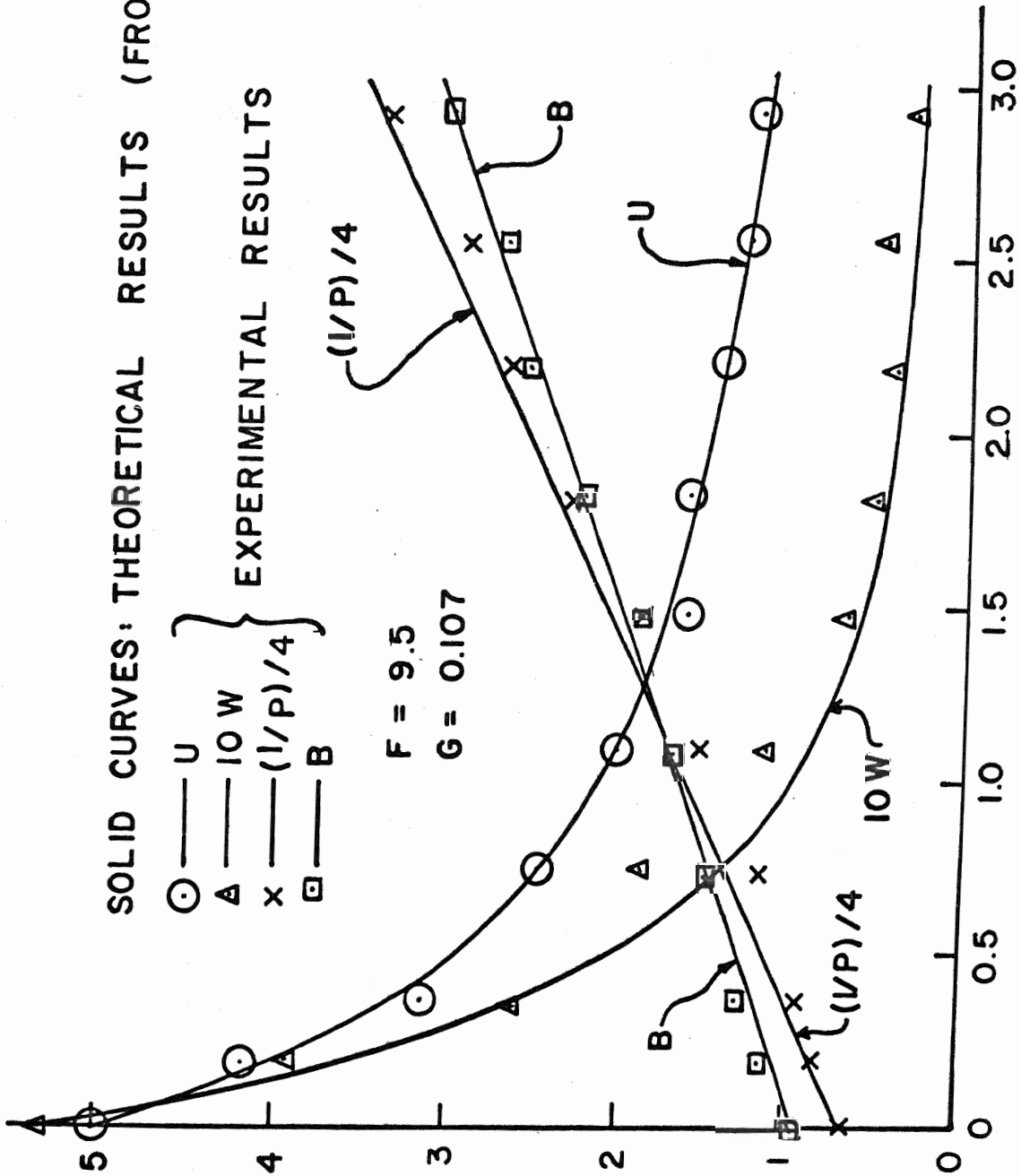


FIGURE 9. COMPARISON OF THEORETICAL AND EXPERIMENTAL RESULTS

DIMENSIONLESS CHARACTERISTIC PLUME RADIUS, B
 DIMENSIONLESS RECIPROCAL OF MAXIMUM BUOYANCY DIVIDED BY FIVE, $(1/P)/5$
 DIMENSIONLESS MAXIMUM SWIRLING VELOCITY MULTIPLIED BY FIFTY, $50W$
 DIMENSIONLESS MAXIMUM AXIAL VELOCITY MULTIPLIED BY FIVE, $5U$

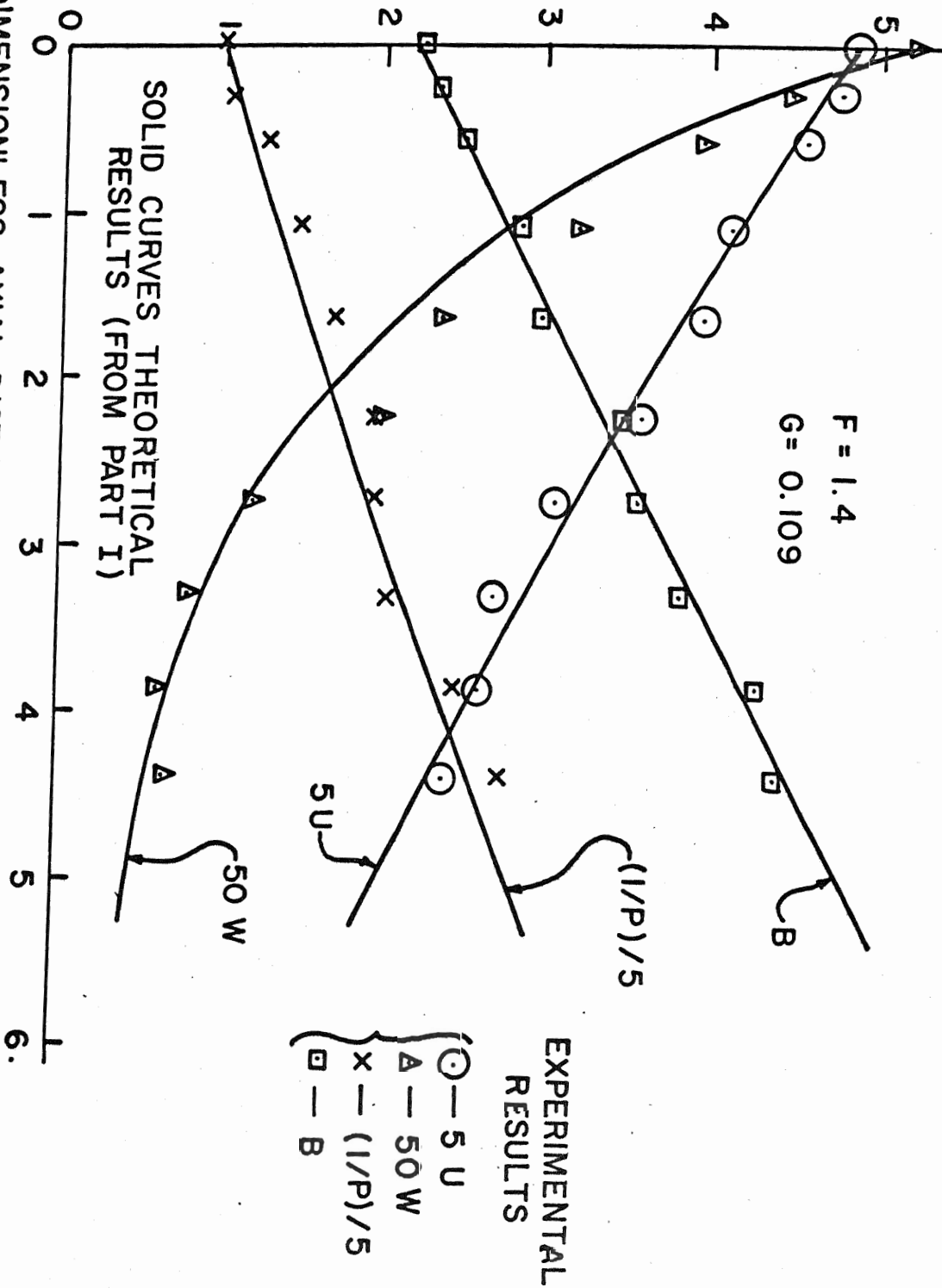


FIGURE 10. COMPARISON OF THEORETICAL AND EXPERIMENTAL RESULTS FOR AN ADDITIONAL PLUME.